



# Stereotactically Injected Kv1.2 and CASPR2 Antisera Cause Differential Effects on CA1 Synaptic and Cellular Excitability, but Both Enhance the Vulnerability to Pro-epileptic Conditions

Timo Kirschstein<sup>1,2,3\*†</sup>, Erika Sadkiewicz<sup>1†</sup>, Gerda Hund-Göschel<sup>1†</sup>, Juliane Becker<sup>1</sup>, Xiati Guli<sup>1</sup>, Steffen Müller<sup>1</sup>, Marco Rohde<sup>1</sup>, Dora-Charlotte Hübner<sup>1</sup>, Hannes Brehme<sup>2</sup>, Stephan Kolbaske<sup>2</sup>, Katrin Porath<sup>1</sup>, Tina Sellmann<sup>1</sup>, Annette Großmann<sup>4</sup>, Matthias Wittstock<sup>2</sup>, Steffen Syrbe<sup>5</sup>, Alexander Storch<sup>2,3</sup> and Rüdiger Köhling<sup>1,3</sup>

## OPEN ACCESS

### Edited by:

Ka Wan Li,  
Vrije Universiteit Amsterdam,  
Netherlands

### Reviewed by:

Nikhil J. Pandya,  
Roche (Switzerland), Switzerland  
Aleksy V. Zaitsev,  
Institute of Evolutionary Physiology  
and Biochemistry (RAS), Russia

### \*Correspondence:

Timo Kirschstein  
timo.kirschstein@uni-rostock.de

<sup>†</sup>These authors have contributed  
equally to this work

**Received:** 02 October 2019

**Accepted:** 06 March 2020

**Published:** 25 March 2020

### Citation:

Kirschstein T, Sadkiewicz E, Hund-Göschel G, Becker J, Guli X, Müller S, Rohde M, Hübner D-C, Brehme H, Kolbaske S, Porath K, Sellmann T, Großmann A, Wittstock M, Syrbe S, Storch A and Köhling R (2020) Stereotactically Injected Kv1.2 and CASPR2 Antisera Cause Differential Effects on CA1 Synaptic and Cellular Excitability, but Both Enhance the Vulnerability to Pro-epileptic Conditions. *Front. Synaptic Neurosci.* 12:13. doi: 10.3389/fnsyn.2020.00013

<sup>1</sup> Oscar Langendorff Institute of Physiology, University of Rostock, Rostock, Germany, <sup>2</sup> Department of Neurology, University of Rostock, Rostock, Germany, <sup>3</sup> Center of Transdisciplinary Neurosciences Rostock, University of Rostock, Rostock, Germany, <sup>4</sup> Institute of Diagnostic and Intervention Radiology, University of Rostock, Rostock, Germany, <sup>5</sup> Clinic for Pediatric and Adolescent Medicine, University of Heidelberg, Heidelberg, Germany

**Purpose:** We present a case of voltage-gated potassium channel (VGKC) complex antibody-positive limbic encephalitis (LE) harboring autoantibodies against Kv1.2. Since the patient responded well to immunotherapy, the autoantibodies were regarded as pathogenic. We aimed to characterize the pathophysiological role of this antibody in comparison to an antibody against the VGKC-associated protein contactin-associated protein-2 (CASPR2).

**Methods:** Stereotactic injection of patient sera (anti-Kv1.2-associated LE or anti-CASPR2 encephalopathy) and a control subject was performed into the hippocampus of the anesthetized rat *in vivo*, and hippocampal slices were prepared for electrophysiological purposes. Using extra- and intracellular techniques, synaptic transmission, long-term potentiation (LTP) and vulnerability to pro-epileptic conditions were analyzed.

**Results:** We observed that the slope of the field excitatory postsynaptic potential (fEPSP) was significantly increased at Schaffer collateral-CA1 synapses in anti-Kv1.2-treated and anti-CASPR2-treated rats, but not at medial perforant path-dentate gyrus synapses. The increase of the fEPSP slope in CA1 was accompanied by a decrease of the paired-pulse ratio in anti-Kv1.2, but not in anti-CASPR2 tissue, indicating presynaptic site of anti-Kv1.2. In addition, anti-Kv1.2 tissue showed enhanced LTP in CA1, but dentate gyrus LTP remained unaltered. Importantly, LTP in slices from anti-CASPR2-treated animals did not differ from control values. Intracellular recordings from CA1 neurons revealed that the resting membrane potential and a single action potential were not different between anti-Kv1.2 and control tissue. However, when the

depolarization was prolonged, the number of action potentials elicited was reduced in anti-Kv1.2-treated tissue compared to both control and anti-CASPR2 tissue. In contrast, polyspike discharges induced by removal of  $Mg^{2+}$  occurred earlier and more frequently in both patient sera compared to control.

**Conclusion:** Patient serum containing anti-Kv1.2 facilitates presynaptic transmitter release as well as postsynaptic depolarization at the Schaffer-collateral-CA1 synapse, but not in the dentate gyrus. As a consequence, both synaptic transmission and LTP in CA1 are facilitated and action potential firing is altered. In contrast, anti-CASPR2 leads to increased postsynaptic potentials, but without changing LTP or firing properties suggesting that anti-Kv1.2 and anti-CASPR2 differ in their cellular effects. Both patient sera alter susceptibility to epileptic conditions, but presumably by different mechanisms.

**Keywords:** limbic encephalitis, voltage-gated potassium channel, synaptic transmission, long-term potentiation, spike frequency adaptation

## INTRODUCTION

Twenty years ago, limbic encephalitis (LE) associated with antibodies against voltage-gated potassium channels (VGKC) was described as a potentially reversible autoimmune encephalitis responding to immunotherapies which was in striking contrast to the formerly known forms of paraneoplastic encephalitis associated with antibodies against intracellular antigens (Buckley et al., 2001). Since VGKC antibodies interfered with the binding of the Kv1 channel blocker dendrotoxin (Hart et al., 2002), VGKC antibodies were believed to bind Kv1 channels. However, it turned out that VGKC antibodies were raised against Kv1-channel complex proteins such as leucine-rich, glioma inactivated 1 (LGI1) and contactin-associated protein-2 (CASPR2) (Lai et al., 2010; Irani et al., 2010). Recently, a large series of sera with VGKC complex antibodies were re-analyzed and only 56% harbored antibodies against LGI1 or CASPR2 (Lang et al., 2017). Almost all of the remaining sera, called double-negative VGKC complex antibody-positive samples, had cytosolic targets, but one serum bound to live hippocampal neurons, suggesting a possible novel surface antigen (Lang et al., 2017).

In this study, we present a case with LE admitted to our emergency presenting with status epilepticus. The patient's serum was double-negative VGKC complex antibody-positive. Further analysis by a commercial laboratory revealed anti-Kv1.2, i.e., a pore-forming subunit of the VGKC Kv1. Since the patient responded well to immunotherapy, the autoantibodies were regarded as pathogenic in nature. In the hippocampus, Kv1.2 channels are particularly present in the middle molecular layer of the dentate gyrus, the CA1 stratum radiatum, and the CA1 stratum lacunosum-moleculare with the most striking immunoreactivity observed on axons and presynaptic terminals (Wang et al., 1993, 1994; Sheng et al., 1994; Monaghan et al., 2001; Gu et al., 2003; Wenzel et al., 2007; Lorincz and Nusser, 2008). Dendritic, but not somatic expression was also reported for cortical and hippocampal pyramidal cells (Sheng et al., 1994; Guan et al., 2006). In contrast, dentate granule cells appeared to be immunonegative (Sheng et al., 1994),

and mossy fibers as well as CA3 pyramidal neurons seem to express Kv1.2 only during ontogenesis at immature stages (Prüss et al., 2010).

Functionally, Kv1.2 encodes a slowly activating and slowly inactivating D-type  $K^+$  conductance when expressed in *Xenopus* oocytes (Stühmer et al., 1989). D-type  $K^+$  currents in central neurons are primarily mediated by Kv1.1 and Kv1.2, both members of the Kv1 channel subfamily. They were recorded from CA1 neurons, and the activation and inactivation curves of D-type  $K^+$  currents cross near the resting membrane potential (RMP) giving rise to a window current (Storm, 1988), hence making this current powerfully regulate the neuron's action potential threshold (Golding et al., 1999; Cudmore et al., 2010). The slow inactivation properties of Kv1 channels, in turn, contribute to spike repolarization (Mitterdorfer and Bean, 2002). Although Kv1.1 is much more widely expressed in the hippocampus than Kv1.2 (Wang et al., 1993, 1994; Veh et al., 1995; Grigg et al., 2000), Kv1.2 knock-out mice die after 15–18 days and are more prone to seizures than mice lacking Kv1.1 (Smart et al., 1998; Brew et al., 2007) supporting the view that Kv1.2 channels are crucial for hippocampal functional integrity. In this study, we injected patient sera containing anti-Kv1.2 or anti-CASPR2 into the rat hippocampus and asked whether synaptic or intrinsic properties were altered in the tissue from these rats.

## MATERIALS AND METHODS

### Case of Kv1.2-Associated Limbic Encephalitis

A 74-year-old male patient was admitted to our emergency with the history of at least two epileptic seizures witnessed by the prehospital emergency medical services. One of these seizures was reported to have presented with a focal onset (orofacial motor symptoms and gaze preference to the left side). Upon initial neurological assessment, he was comatose (Glasgow Coma Scale 3) most likely due to status epilepticus and presented

with tetraparesis, but accentuated at the left side. Therefore, he immediately received endotracheal intubation and mechanical ventilation. Computed tomography was inconclusive, the further clinical and paraclinical work-up revealed inflammation (leukocytes 9500/ $\mu$ l; C-reactive protein 90  $\mu$ mol/l) which was suspected to be associated with aspiration pneumonia, but electrolytes as well as renal and hepatic function did not explain the patient's clinical situation. The subsequently performed MRI found hyperintense cortices in the right hemisphere, in particular the temporal lobe which was attributed to status epilepticus or encephalitis (**Figure 1**). The EEG showed epileptic discharges on right hemispheric leads (**Figure 1**). Hence, we started to treat the patient with levetiracetam and propofol for sedation. Analysis of the cerebrospinal fluid showed increased protein and lactate levels, but could not evidence an acute infectious inflammation (leukocytes 1/ $\mu$ l, lactate 4 mmol/l, protein 520 mg/l, albumin 370 mg/l, negative for intrathecal immunoglobulin synthesis, identical oligoclonal bands in CSF and serum, i.e., type IV reaction). Neurotropic viruses (HSV, VZV, CMV, and EBV) as well as Lyme neuroborreliosis were also ruled out. Given the suspected LE, we tested a battery of autoantibodies and found a positive titer for antibodies against VGKCs (115 pmol/l). Unexpectedly, anti-LG1 was negative, but a novel antibody, IgG against the pore-forming subunit KCNA2 (also called Kv1.2), could be detected (titer 1:10, Euroimmun, Lübeck, Germany). The patient received five episodes of plasmapheresis, and subsequently recovered from comatose state and spontaneously opened his eyes. We received blood serum samples together with the permission to keep these samples in  $-20^{\circ}\text{C}$  for further scientific studies. The patient was supplied with a percutaneous endoscopic gastrostoma as well as a tracheostoma and was successfully transferred to rehabilitation 4 weeks after admission.

### Case of Anti-CASPR2 Encephalopathy

A 1-year and 8 months old boy was admitted for change of behavior with unprovoked crying, suspected pain, and severe sleeplessness. He developed treatment refractive hypertension and general weakness. Brain MRI, whole body MRI and laboratory work-up was unremarkable. Cerebrospinal fluid analysis showed mild pleocytosis (12 leucocytes, normal protein, no oligoclonal bands). Neurotropic viruses and neuroborreliosis were ruled out. Testing for antineural antibodies revealed high titer anti-CASPR2 (1:1280) in serum only (VGKC 119 pmol/l). Electrophysiological studies with nerve conduction studies and EEG were normal. Pediatric Morvan syndrome was diagnosed and he received treatment with intravenous immunoglobulins and repeated methylprednisolone pulses which resulted in resolution of acute symptoms. At 3 years of age, he was diagnosed with autism spectrum disorder. The patient's clinical and serological findings were reported within a series of children with CASPR2 autoimmunity (Syrbe et al., 2020).

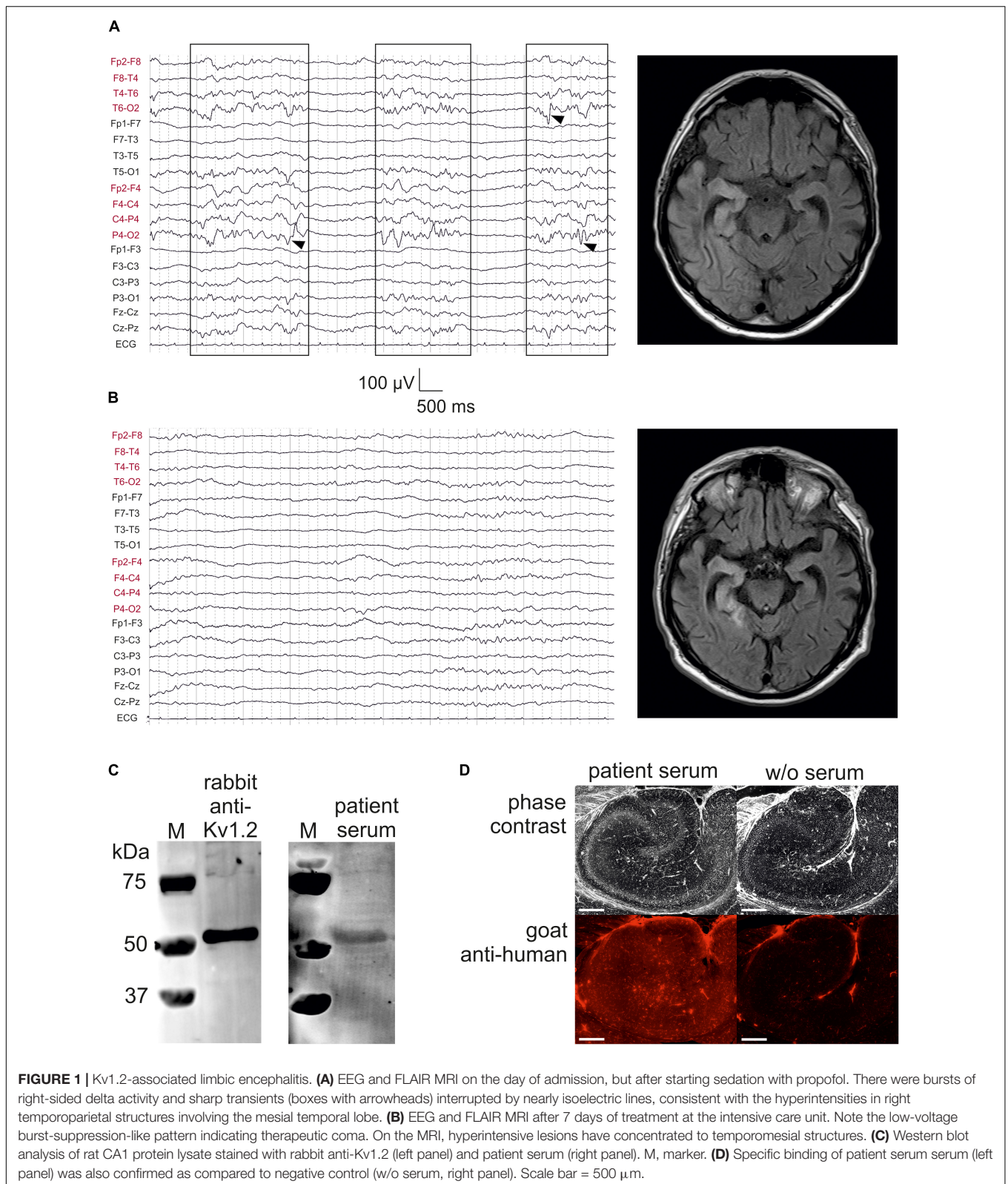
### Stereotactic Intrahippocampal Serum Injection *in vivo*

Stereotactic injection of the serum from the case patients or a non-epileptic control subject into both hippocampi *in vivo*

was performed as previously described (Blome et al., 2018; Kersten et al., 2019). Briefly, 75 male Wistar rats (8–10 weeks old, Charles River, Sulzfeld, Germany) were anesthetized with S-ketamine (100 mg/kg i.p.) and xylazine (15 mg/kg i.p.) and mounted on a stereotactic frame (Narishige, Tokyo, Japan). Using a Hamilton syringe (75N; Hamilton AG, Bonaduz, Switzerland) patient or control serum was slowly (10 steps of 0.5  $\mu$ l every 2 min, total of 5  $\mu$ l for each side) injected into the hippocampus with the following coordinates: 5.2 mm posterior,  $\pm 4.3$  mm lateral, 4.8 mm deep (relative to bregma). These coordinates were obtained in previous studies (Blome et al., 2018; Kersten et al., 2019). After completing the injection, the syringe remained *in situ* for another 2 min to enable proper serum diffusion into the hippocampus. After surgery, rats were given metamizole (100–150 mg/kg) for postoperative pain control and allowed to recover in an atmosphere with enhanced oxygen fraction (4–5 l/min in an 8 l glass vessel). There was one rat (anti-Kv1.2 group) showing severe respiratory insufficiency and was thus killed during anesthesia, but no further severe morbidity or mortality was observed (overall lethality 1/98). Due to the randomization process, rats treated with anti-Kv1.2, anti-CASPR2 or control serum did not differ significantly in weight during surgery (anti-Kv1.2:  $256 \pm 10$  g,  $n = 36$ ; control:  $265 \pm 10$  g,  $n = 39$ ; anti-CASPR2:  $298 \pm 12$  g,  $n = 23$ ) or in latency between surgery and slice preparation (anti-Kv1.2:  $2.6 \pm 0.3$  days; control:  $3.1 \pm 0.4$  days; anti-CASPR2:  $3.6 \pm 0.5$  days). Moreover, experimenters were blinded to the injected serum (whether anti-Kv1.2, anti-CASPR2 or control serum). In addition, we also used 11 naive, non-operated rats for input–output relations and long-term zero  $\text{Mg}^{2+}$  experiments as a second control. All procedures were performed according to national and international guidelines on the ethical use of animals (European Council Directive 86/609/EEC, approval of local authority LALLF M-V/TSD/7221.3-1.1-017/11 and M-V/TSD/7221.3-1.1-007/16), and all efforts were made to minimize animal suffering and to reduce the number of animals used.

### Immunodetection of Anti-Kv1.2 in Patient Serum

The immunoreactivity of patient serum was tested by immunofluorescence and Western blot analysis. To this end, hippocampal brain slices of adult male Wistar rats were obtained and either used for immunofluorescence or Western blot. In order to increase the protein content of the IgG fraction, the patient serum was concentrated by a factor of 4 with centrifugal concentrators (Vivaspin) using a 100 kDa molecular weight cutoff filter to omit the albumin fraction. For Western blot analysis, the hippocampal tissue was homogenized in RIPA buffer to disrupt cells. The crude extract was centrifuged to yield a clear protein solution. Performing SDS gel electrophoresis, a total of 15  $\mu$ g proteins were separated and blotted onto PVDF membranes (Immobilon-FL, Millipore). Overnight incubation with a commercial rabbit polyclonal anti-Kv1.2 antibody (1:1000, Alomone, #APC-010) or patient serum was followed by secondary antibody reaction (anti-human or anti-rabbit IRDye 800CW, Odyssey). Specific proteins band were



visualized using the Odyssey infrared imaging scanner (Li-cor). For immunofluorescence staining, the slices were fixed in 3.7% formaldehyde solution, then cryo-preserved with 30% buffered

sucrose solution at 4°C overnight and finally frozen. Thin layers of 50  $\mu$ m thickness were sliced using a cryo-vibratome and mounted on microscope object carriers. Immunoreaction was

carried out with or without patient serum (negative control). Fluorescence signals emerged from Cy5-coupled secondary antibodies (goat anti-human, Invitrogen) and were visualized using a Leica DMI 6000B fluorescence microscopy under identical conditions. Each image was taken in a tile scan mode to receive an overview picture from the hippocampus.

## Electrophysiological Recordings and LTP Induction

Hippocampal slices were prepared 1 to 6 days after stereotactic surgery (Blome et al., 2018; Kersten et al., 2019). Briefly, rats were decapitated in deep anesthesia with diethyl ether, the brains were rapidly removed and submerged into oxygenated ice-cold dissection solution containing (in mM) 125 NaCl, 26 NaHCO<sub>3</sub>, 3 KCl, 1.25 NaH<sub>2</sub>PO<sub>4</sub>, 0.2 CaCl<sub>2</sub>, 5 MgCl<sub>2</sub> and 13 D-glucose (95% O<sub>2</sub>, 5% CO<sub>2</sub>; pH 7.4; 306–314 mosmol/kg). Horizontal hippocampal brain slices (400 μm) were cut using a vibratome (Campden Instruments, Loughborough, United Kingdom), and slices were then transferred into a holding chamber containing artificial cerebrospinal fluid (ACSF) containing (in mM) 125 NaCl, 26 NaHCO<sub>3</sub>, 3 KCl, 1.25 NaH<sub>2</sub>PO<sub>4</sub>, 2.5 CaCl<sub>2</sub>, 1.3 MgCl<sub>2</sub> and 13 D-glucose (306–314 mosmol/kg, bubbled with 95% O<sub>2</sub> and 5% CO<sub>2</sub> to maintain the pH at 7.4).

Synaptic transmission and plasticity were assessed by recording field excitatory postsynaptic potentials (fEPSPs) from CA1 or from the dentate gyrus. The slices were continuously bathed in oxygenated ACSF (flow rate of 2 ml/min, temperature 32 ± 1°C, npi electronic GmbH, Tamm, Germany). For stimulation of the afferent fibers (Schaffer collaterals, or medial perforant path, respectively), bipolar stimulating electrodes fabricated from teflon-insulated platinum wire electrodes (PT-2T, Science Products, Hofheim, Germany) were placed into CA1 stratum radiatum or dentate gyrus middle molecular layer, respectively. Stimuli were delivered through a stimulus isolator (A365, World Precision Instruments, Sarasota, FL, United States) triggered by a Master-8 stimulator (A.M.P.I., Jerusalem, Israel), and the stimulus intensity was routinely increased from 25 to 300 μA. For the prospective analysis of fEPSP slopes (Figure 3C), we adjusted the stimulus intensity in each slice to the half-maximum amplitude, which was typically around 85 μA (between 75 and 125 μA). The same procedure was done to establish the baseline stimulus intensity for LTP experiments. NMDAR-dependent LTP was induced by a paradigm consisting of 10 trains of 20 stimuli at 100 Hz (stimulus duration 100 μs, intertrain interval 800 ms, at double baseline stimulation intensity, Blome et al., 2018; Kersten et al., 2019). NMDAR-independent LTP was induced by a similar paradigm (stimulus duration 100 μs, intertrain interval 800 ms, at double baseline stimulation intensity), but in the presence of D-AP5 (50 μM). Recording electrodes filled with ACSF were placed into CA1 stratum radiatum or dentate gyrus middle molecular layer, respectively. Analog recording signals were amplified, filtered at 1 kHz by an EXT-10-2F (npi electronic GmbH, Tamm, Germany), and digitized with a Micro1401 analog-to-digital converter (Cambridge Electronic Design, Cambridge, United Kingdom) using Signal 2.16 software (Cambridge Electronic Design, Cambridge, United Kingdom).

Chemicals used for physiological solutions were purchased from Sigma-Aldrich (Taufkirchen, Germany).

Intracellular recordings were performed in CA1 pyramidal cells impaled with borosilicate glass microelectrodes (80–120 MΩ, pulled with Sutter P-97 and filled with 3 M potassium acetate and 0.013 M KCl) using an SEC-10LX amplifier (npi electronic). In these recordings, RMP was determined, and action potentials were elicited by short (duration 7 ms, from +0.5 to +2.4 nA in 0.1-nA-steps, interstimulus-interval 1.1 s) or prolonged current injections (duration 600 ms, from –1.0 to +1.0 nA in 0.1-nA-steps, interstimulus interval 10 s). Action potential (AP) threshold was assessed as the voltage at the point of the steepest slope of the AP upstroke (i.e., the beginning of the upstroke). We also determined AP amplitude, AP overshoot, and AP duration at half-maximum amplitude (width at half), and the afterhyperpolarizing potential following prolonged depolarization (600 ms, +1.0 nA). Digitization at 10 kHz and offline data processing were performed with the CED package (Micro1401 analog-to-digital converter, Signal 2.16 software, all from Cambridge Electronic Design, Cambridge, United Kingdom).

## Acutely Induced Epileptiform Discharges

In order to test the effect of anti-Kv1.2 on acutely induced epilepsy, we evoked spontaneous epileptic discharges by removal of Mg<sup>2+</sup> from the bath. In these experiments, the extracellular electrode was placed in the upper blade of the dentate gyrus molecular layer. At the beginning of each experiment, the absence of spontaneous epileptic discharges was confirmed by recording under baseline conditions for at least 20 min. Then Mg<sup>2+</sup> was omitted from the ACSF, and the recordings were maintained for further 60 min. Spontaneous epileptic events were counted in each slice for the entire recording period of 80 min. Occasionally, epileptic events consisted of more than one spike discharge. In a second approach, these polyspike discharges were analyzed individually. Further events, such as seizure-like episodes or spreading depressions, were also documented.

## Statistical Analysis

Data are expressed as mean values ± the standard error of the mean (SEM) or box-whisker plots (created with SigmaStat 3.5: box = quartiles, whiskers = 10/90% percentiles). For statistical evaluation, data were first tested for normal distribution and equal variance (SigmaStat 3.5). Depending on this normality test, statistical comparisons were performed either using parametric (paired or unpaired *t*-test, ANOVA) or non-parametric tests (Mann-Whitney test) as indicated. The level of significance is indicated by asterisks (\**P* < 0.05, \*\**P* < 0.01).

## RESULTS

We present a case with status epilepticus due to anti-Kv1.2-associated LE, presenting with lateralized delta activity as well as sharp transients, predominantly over right posterior hemispheric leads (Figure 1A, left panel). Bursts of focal slowing and epileptiform potentials (boxes with arrowheads in Figure 1A)

were interrupted by nearly isoelectric lines as a result from propofol medication in the mechanically ventilated patient (burst-suppression pattern). FLAIR MRI at this time point clearly showed high signal intensities on the right temporoparietal lobes with strong involvement of temporomesial structures (**Figure 1A**, right panel), consistent with the right-sided epileptic activity. One week later, these hyperintense lesions tended to concentrate on these temporomesial structures providing *post hoc* evidence for the LE (**Figure 1B**, right panel). The EEG at this time point showed typical burst-suppression due to therapeutic coma rather than lateralized epileptic activity (**Figure 1B**, left panel).

To test the specificity of the patient serum, we performed a Western blot analysis using rat CA1 hippocampal protein lysate immunoblotted with rabbit anti-Kv1.2 which detected a band consistent with the expected molecular weight of rat Kv1.2 (499 amino acids, 57 kDa; **Figure 1C**, left panel). When this primary antibody was replaced by concentrated albumin-free patient serum counterstained by an anti-human secondary antibody, the same band was obtained (**Figure 1C**, right panel). Importantly, there were no further bands in this blot suggesting that the predominant protein identified by the patient serum presumably represented Kv1.2. Immunohistochemistry on a rat hippocampal section confirmed that albumin-free patient serum (**Figure 1D**, left panel) showed specific binding as compared to the negative control without serum (**Figure 1D**, right panel).

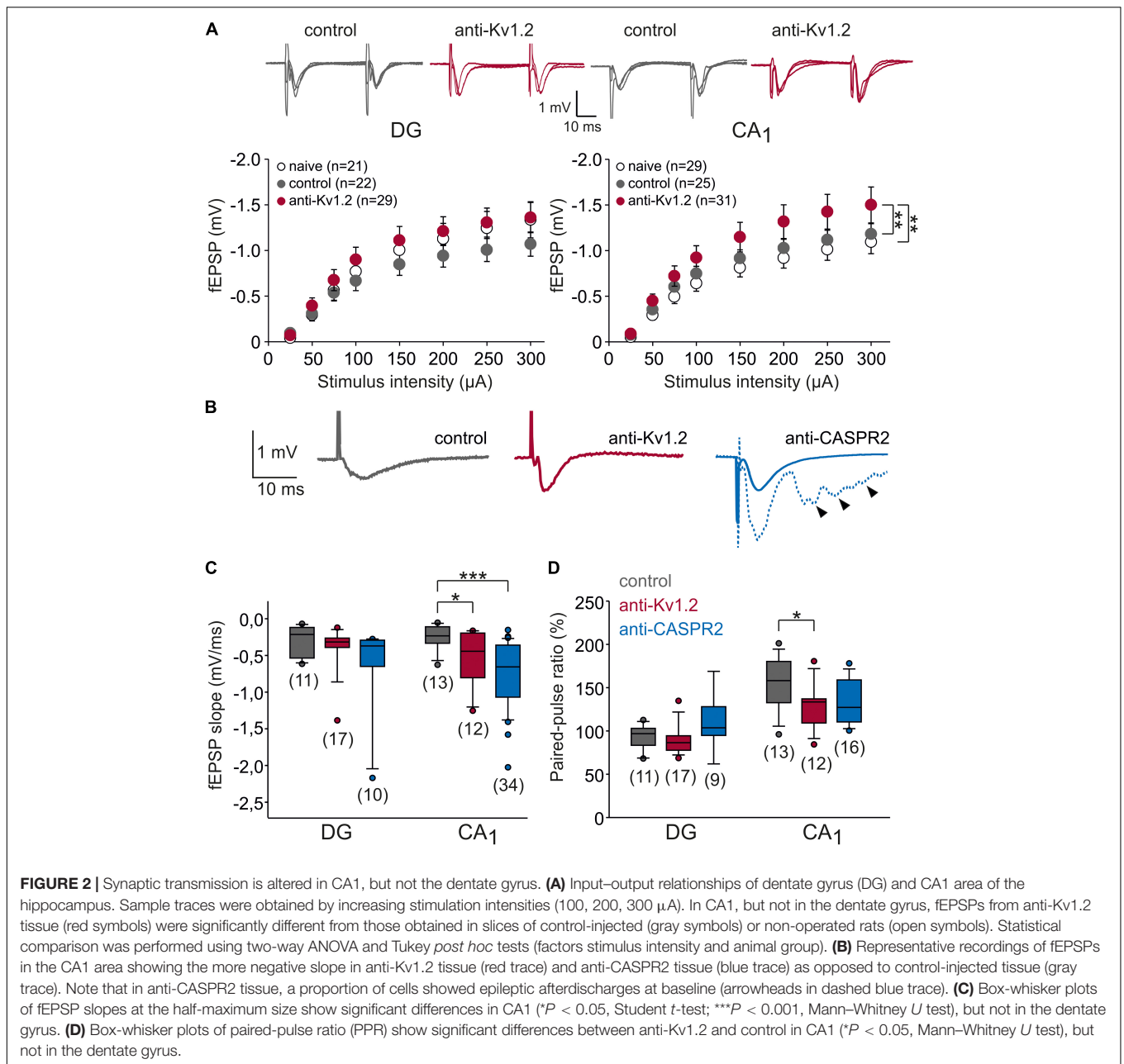
## Pre- and Postsynaptic Excitability and Plasticity

In this study, we aimed to study the effects of patient serum containing anti-Kv1.2 on synaptic function. To this end, we stereotactically injected serum into the hippocampus *in vivo* and obtained horizontal hippocampal brain slices 1–6 days after surgery. We studied the Schaffer collateral-CA1 synapse and the medial perforant path-dentate gyrus synapse, both typical expression sites of Kv1.2. Increasing stimulation intensities (25 to 300  $\mu$ A) of the afferent fibers led to increasing excitatory postsynaptic field potentials (fEPSPs) in the respective hippocampal area (**Figure 2A**). Obviously, two-way ANOVA revealed a significant effect of stimulus intensity ( $P < 0.01$  in both fields), but there was no significant interaction between stimulus intensity and animal group ( $P < 0.9$  in both fields). While input–output relations did not show consistent significant differences for anti-Kv1.2 in the dentate gyrus (Tukey *post hoc* test:  $P < 0.05$  between control and anti-Kv1.2, but  $P = 0.429$  between naive and anti-Kv1.2), there was a consistent group effect in the CA1 area (Tukey *post hoc* test:  $P = 0.01$  between anti-Kv1.2 and control as well as between anti-Kv1.2 and naive tissue, **Figure 2A**). Since we observed that the slope of the fEPSP recorded in CA1 was more negative in slices from anti-Kv1.2-treated than in control-injected rats (**Figure 2B**), we performed a further series of experiments and selected the half-maximum fEPSP of each experiment in order to determine the slope of this potential. As shown in **Figure 2C**, the negative slope of the half-maximum fEPSP in anti-Kv1.2-treated tissue was indeed significantly higher than in controls at Schaffer-collateral-CA1 synapses (anti-Kv1.2:  $P < 0.05$ , Student *t*-test),

but not in the dentate gyrus ( $P = 0.323$ , Mann–Whitney *U* test). Since we aimed to compare anti-Kv1.2 effects with anti-CASPR2 effects, we used a further patient serum containing CASPR2 autoantibodies. In anti-CASPR2-treated tissue, the slope of the fEPSP was highly variable and, occasionally, we obtained fEPSPs with epileptic afterdischarges (38% of anti-CASPR2 slices, see arrowhead in rightmost traces, **Figure 2B**). Hence, the negative slope of the half-maximum fEPSP in this tissue was significantly higher than in control slices ( $P < 0.001$ , Mann–Whitney *U* test, **Figure 2C**) indicating enhanced synaptic transmission under both pathological conditions, but suggesting differences between anti-Kv1.2 and anti-CASPR2.

Increased fEPSP slopes may suggest a more synchronous transmitter release, for instance by an inhibitory effect of anti-Kv1.2 on presynaptic terminals, because Kv1 channels were reported to dampen presynaptic post-firing hyperexcitability (Dodson et al., 2003). One measure to address this question is to test paired-pulse plasticity. Since transmitter release probability is inversely related to the paired-pulse ratio (PPR; Zucker, 2002), we delivered paired pulses (interstimulus interval 40 ms). As expected, the PPR of fEPSP slopes in the dentate gyrus was not significantly altered (anti-Kv1.2:  $89 \pm 4\%$ ,  $n = 16$ ; control:  $92 \pm 4\%$ ,  $n = 11$ ;  $P = 0.608$ ; Mann–Whitney *U* test; **Figure 2D**), but confirmed the typical paired-pulse depression in the medial perforant path (Dietrich et al., 1997). In contrast, slices from anti-CASPR2-treated animals showed paired-pulse facilitation rather than depression ( $110 \pm 9\%$ ,  $n = 9$ , **Figure 2D**) which could suggest that anti-CASPR2 leads to presynaptic inhibition at medial perforant path terminals. In contrast, we obtained significantly reduced PPR of fEPSP slopes in the CA1 area from anti-Kv1.2 tissue as compared to control (anti-Kv1.2:  $129 \pm 7\%$ ,  $n = 12$ ; control:  $153 \pm 8\%$ ,  $n = 13$ ;  $P < 0.05$ , Mann–Whitney *U* test; **Figure 2D**), suggesting an increased transmitter release probability at these synapses. The PPR in anti-CASPR2 slices was only slightly reduced ( $133 \pm 6\%$ ,  $n = 16$ ,  $P = 0.076$  versus control, Mann–Whitney *U* test; **Figure 2D**) indicating that the increased fEPSP slope in this tissue was partially due to increased presynaptic transmitter release, but may have involved other mechanisms such as network disinhibition.

So far, these data suggest that anti-Kv1.2 and anti-CASPR2 differ in their effects on Schaffer collateral presynaptic function. However, they cannot exclude that postsynaptic cells may also be altered in anti-Kv1.2 or anti-CASPR2 tissue. To control for this, we performed intracellular recordings of CA1 neurons from anti-Kv1.2, anti-CASPR2 and control rats. At first, there were no significant differences in the RMP and cellular membrane properties such as resistance and time constant between anti-Kv1.2 and controls (**Table 1**), indicating that anti-Kv1.2 did not significantly affect the leak conductance. When we applied short current injections to elicit a single action potential (duration 7 ms, interstimulus interval 1.1 s), there were again no differences in action potential characteristics (**Table 1**) arguing against major postsynaptic differences in intrinsic cellular excitability between these two groups. In contrast, cells from anti-CASPR2 tissue differed from cells recorded in control or anti-Kv1.2-treated slices (**Table 1**). It is important to note, however, that all significant

**TABLE 1 |** Intrinsic CA1 pyramidal cell properties.

	Control (n = 9)	Anti-Kv1.2 (n = 11)	Anti-CASPR2 (n = 9)
Resting membrane potential	$-58.4 \pm 1.2$ mV	$-59.1 \pm 1.6$ mV	$-62.5 \pm 1.3$ mV
Membrane resistance	$45.7 \pm 3.7$ M $\Omega$	$43.1 \pm 6.3$ M $\Omega$	$39.7 \pm 3.8$ M $\Omega$
Membrane time constant*	$7.3 \pm 0.7$ ms	$8.3 \pm 0.6$ ms	$10.2 \pm 0.8$ ms (a)
Action potential amplitude	$65.9 \pm 2.0$ mV	$64.1 \pm 2.4$ mV	$67.8 \pm 1.3$ mV
Action potential overshoot	$6.6 \pm 1.1$ mV	$4.5 \pm 2.2$ mV	$3.3 \pm 1.8$ mV
Action potential width at half*	$1.6 \pm 0.1$ ms	$1.6 \pm 0.1$ ms	$1.4 \pm 0.05$ ms (a,b)
Action potential threshold*	$-45.1 \pm 1.3$ mV	$-43.8 \pm 2.4$ mV	$-51.0 \pm 1.9$ mV (a,b)
Afterhyperpolarizing potential*	$-6.3 \pm 0.9$ mV	$-5.9 \pm 1.1$ mV	$-13.6 \pm 1.5$ mV (a,b)

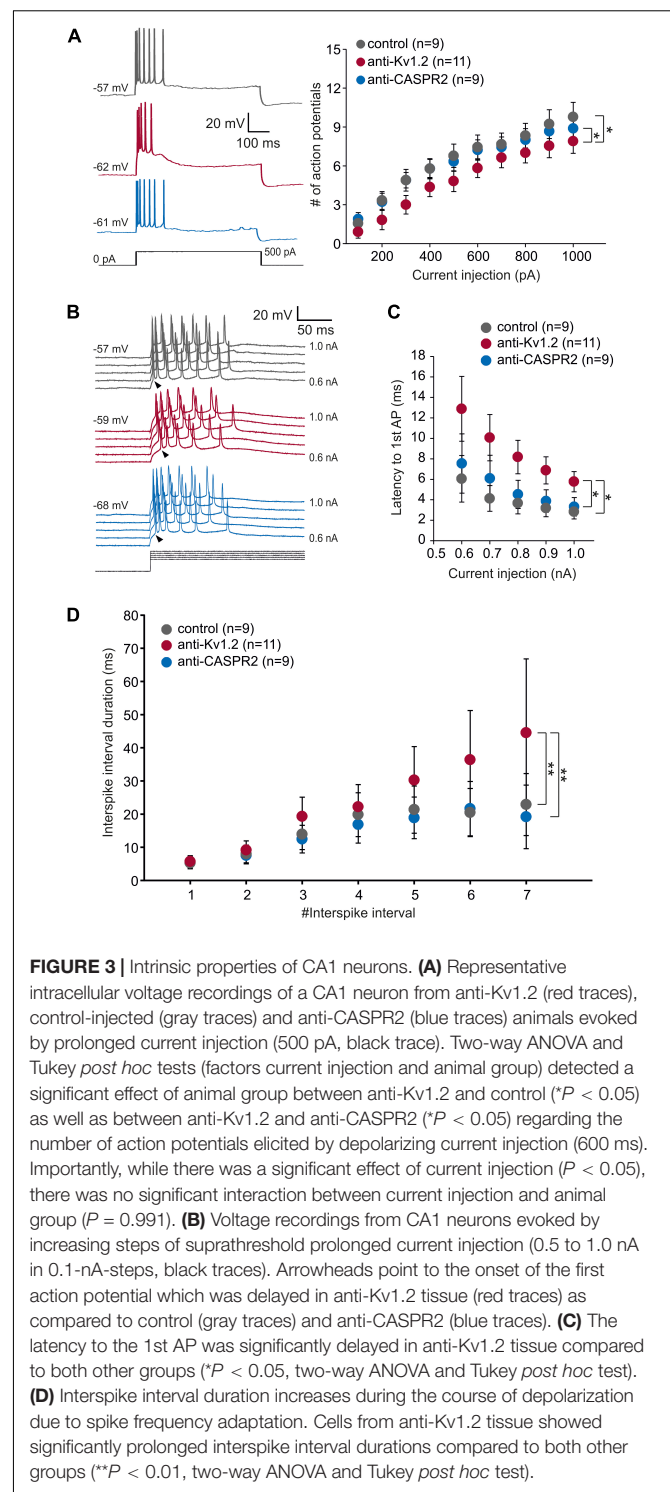
Statistical comparisons were performed using ANOVA with Student–Newman–Keuls *post hoc* tests. Significant group effects are indicated with asterisks, the lowercase letters in parentheses indicate statistically significant differences between anti-CASPR2 and control (a), or between anti-CASPR2 and anti-Kv1.2 (b).

differences obtained (especially action potential characteristics and afterhyperpolarizing potential) are not compatible with an impaired  $K^+$  channel function of CA1 neurons, but may rather indicate separate changes on the network level.

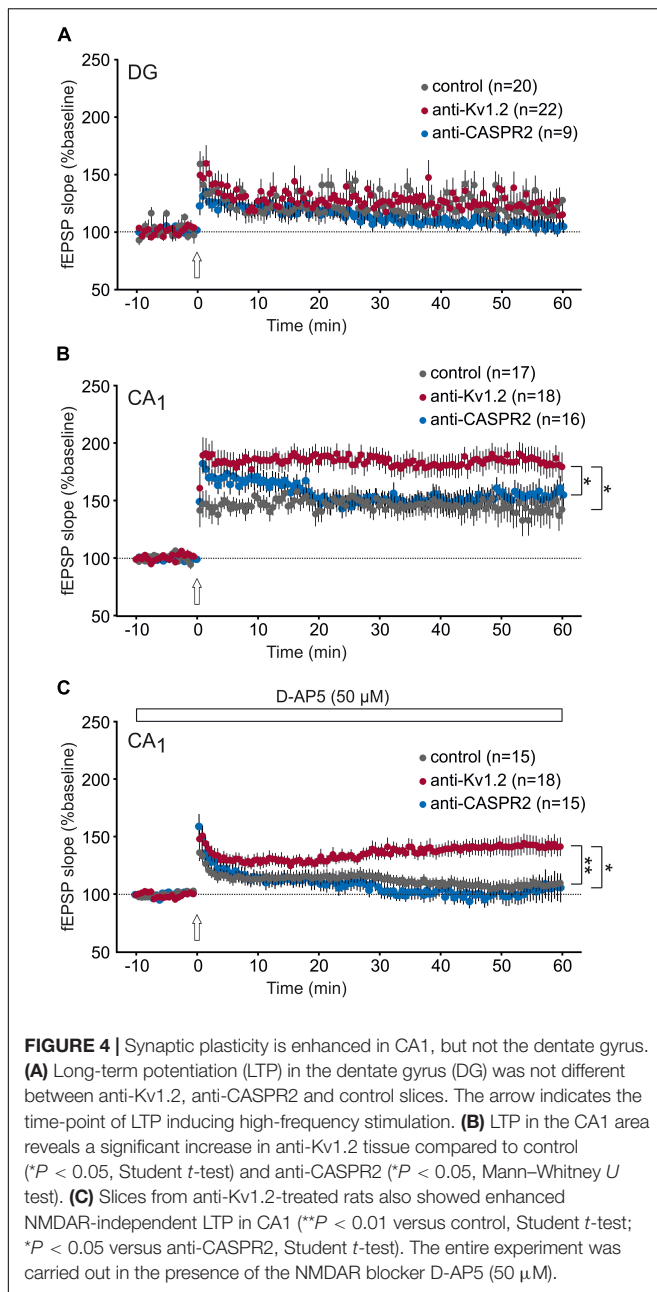
In addition, one unique property of Kv1.2, but not of other Kv1 channels, is the use-dependent activation (Baronas et al., 2015). Hence, we prolonged the current injection to 600 ms (500 pA) with an interstimulus interval of 10 s. Under these conditions, we observed that CA1 cells from anti-Kv1.2 showed a significantly reduced number of action potentials compared to control ( $P < 0.05$ , two-way ANOVA with factors current injection and animal group, followed by Tukey *post hoc* test; **Figure 3A**). Importantly, there was also a significant difference between anti-Kv1.2 and anti-CASPR2 ( $P < 0.05$ ; **Figure 3A**), while there was no significant interaction between current injection and animal group ( $P = 0.991$ , two-way ANOVA). However, spike broadening was not different between all experimental groups as assessed by the action potential duration (width at half: 3rd AP relative to 1st:  $168 \pm 51\%$ ,  $n = 11$  in anti-Kv1.2;  $178 \pm 59\%$ ,  $n = 9$  in control;  $176 \pm 59\%$ ,  $n = 9$  in anti-CASPR2;  $P = 0.369$ , one-way ANOVA).

Intriguingly, we also noticed that the first action potential occurred later in anti-Kv1.2-treated than in control tissue (see arrowheads in **Figure 3B**). This was a consistent finding, CA1 neurons from anti-Kv1.2 tissue showed significantly higher latencies to the first action potential compared to both control and anti-CASPR2 tissue ( $P < 0.05$ , two-way ANOVA with factors current injection and animal group, followed by Tukey *post hoc* test; **Figure 3C**). In addition, we analyzed the interspike interval duration during current injection (600 ms, +1.0 nA) and found significantly prolonged interspike intervals in cells from anti-Kv1.2-treated rats as compared to both other groups ( $P < 0.01$  versus control and anti-CASPR2, two-way ANOVA with factors #interspike interval and animal group, followed by Tukey *post hoc* test; **Figure 3D**). Since the delayed firing in anti-Kv1.2 could not be attributed to an altered membrane time constant (**Table 1**), our data suggest that both pre- and postsynaptic sites may be involved in changes observed in anti-Kv1.2 tissue.

Next, we asked whether the level of achievable long-term potentiation (LTP) might be altered in anti-Kv1.2 tissue. Thus, we were interested in the propensity to activate postsynaptic NMDA receptors upon high-frequency extracellular afferent stimulation. Consistent with our previous data so far, LTP at the medial perforant path-dentate gyrus synapse was almost identical between all three groups (anti-Kv1.2:  $120 \pm 11\%$ ,  $n = 22$ ; control:  $120 \pm 13\%$ ,  $n = 20$ ; anti-CASPR2:  $104 \pm 5\%$ ,  $n = 9$ ; **Figure 4A**), but in marked contrast, CA1-LTP in anti-Kv1.2-treated tissue ( $182 \pm 11\%$ ,  $n = 18$ ) was significantly higher as compared to both control ( $143 \pm 14\%$ ,  $n = 17$ ,  $P < 0.05$ , Student *t*-test) and anti-CASPR2 tissue ( $155 \pm 10\%$ ,  $n = 16$ ,  $P < 0.05$ , Mann-Whitney *U* test; **Figure 4B**). In addition, we also tested NMDAR-independent LTP at Schaffer collateral-CA1 synapses which was again significantly enhanced in slices from anti-Kv1.2-treated rats ( $143 \pm 10\%$ ,  $n = 18$ ; control:  $109 \pm 6\%$ ,  $n = 15$ ,  $P < 0.01$ , Student *t*-test; anti-CASPR2:  $106 \pm 13\%$ ,  $n = 15$ ,  $P < 0.05$ , Student *t*-test; **Figure 4C**). Taken together, these findings suggest that stereotactic injection with patient serum containing anti-Kv1.2 facilitates presynaptic transmitter release



and postsynaptic depolarization at the Schaffer collateral-CA1 synapse, but not in the dentate gyrus, and as a consequence of this, both synaptic transmission and LTP in CA1 are facilitated. In contrast, patient serum containing anti-CASPR2 enhances postsynaptic responses, but rather independently of  $K^+$  channel modulation, and does not interfere with LTP at Schaffer collateral-CA1 synapses.



## Vulnerability to Epileptic Conditions

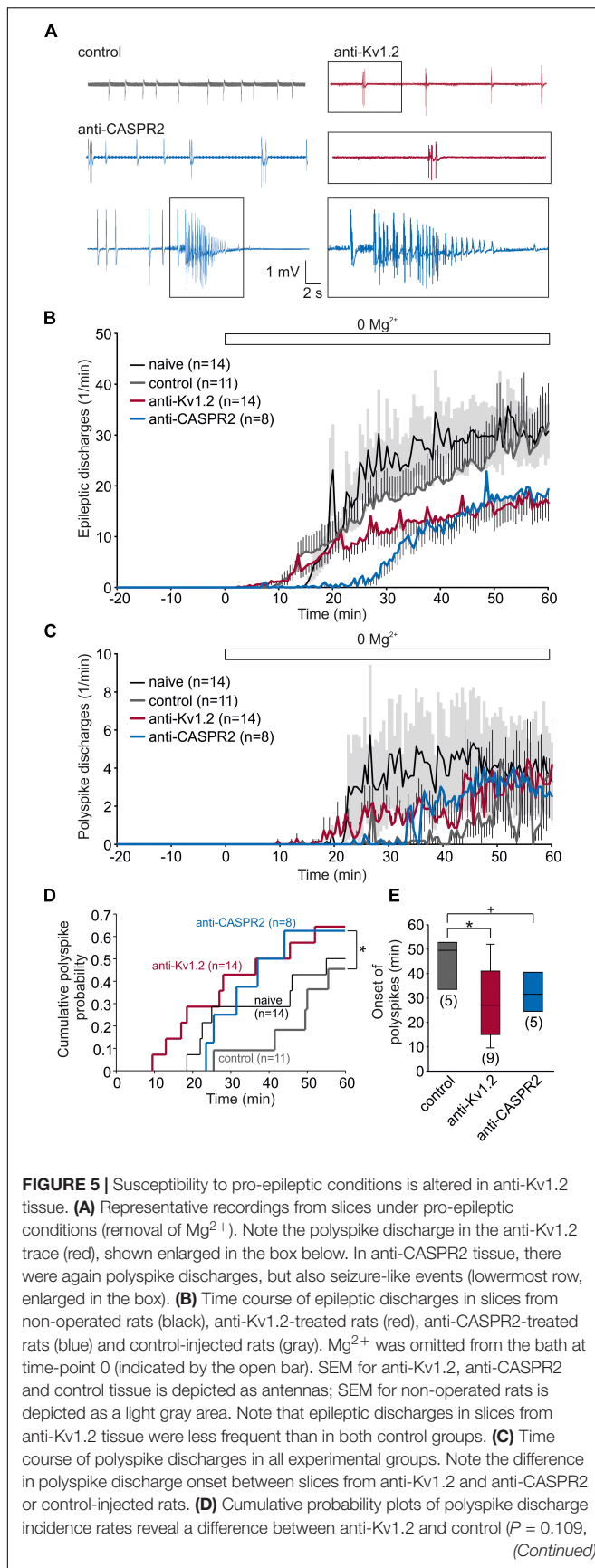
Facilitation of synaptic transmission and plasticity may imply that the tissue might be more vulnerable to hyperexcitable states. Since the anti-Kv1.2 encephalitis suffered from epilepsy, we tested the susceptibility of anti-Kv1.2-treated and anti-CASPR2-treated tissue by removal of  $Mg^{2+}$  from the bath. Under these conditions, spontaneous epileptiform potentials were elicited in all experimental groups (Figure 5A). In fact, there was a tendency toward more epileptic events in control tissue, albeit not significant (Figure 5B). While the vast majority of epileptic events consisted of a single interictal spike, we occasionally observed two or more spikes (referred to as polyspike discharges)

and, intriguingly, the incidence of these polyspike discharges was markedly higher in slices from anti-Kv1.2-treated and anti-CASPR2-treated rats (Figure 5C). In order to quantify the development of polyspike discharges, we determined the cumulative probability of polyspike discharge incidence rates showing a trend toward a shorter latency and a higher proportion in anti-Kv1.2 tissue ( $P = 0.109$ , Kaplan–Meier log-rank test) and anti-CASPR2 tissue ( $P = 0.05$ , Kaplan–Meier log-rank test, Figure 5D). When only slices with polyspike discharges were analyzed, the onset of these discharges was significantly advanced in anti-Kv1.2 as compared to control ( $P < 0.05$ , Mann–Whitney *U* test; Figure 5E). These data indicate that susceptibility to epileptic conditions was altered in anti-Kv1.2 tissue. The onset of polyspike discharges in anti-CASPR2 tissue tended to be also advanced ( $P = 0.095$ , Mann–Whitney *U* test; Figure 5E), but more intriguingly, this tissue was markedly prone to seizure-like events (see blue sample traces in Figure 5A) which were never observed in the other groups (anti-CASPR2: 4/8 slices,  $P < 0.05$  versus anti-Kv1.2 and control, Fisher’s exact test).

## DISCUSSION

We present a case of Kv1.2-associated LE with status epilepticus. We took advantage of testing this patient’s serum by stereotactic injection into the rat hippocampus. The human Kv1.2 protein primary structure is 99.4% identical to the rat isoform (NCBI, blast analysis). Therefore, we assumed that the human antibody could bind to the rat Kv1.2 in the hippocampus, and using Western blot we showed that both a commercial rabbit anti-Kv1.2 and the patient’s serum detected the same band which was consistent with the calculated molecular weight of 57 kDa for this protein. We also had the opportunity to compare this patient’s serum with a serum from a case of anti-CASPR2 encephalopathy. This approach was also used with patient cerebrospinal fluid containing NMDAR or GAD65 antibodies in previous studies (Hackert et al., 2016; Würdemann et al., 2016; Blome et al., 2018; Kersten et al., 2019). Thus, we propose the intrahippocampal bolus injection of serum is also a valid model for studying patient-derived autoantibodies.

Originally, Kv1 shaker-related  $K^+$  channels have been characterized pharmacologically by the use of dendrotoxins, relatively selective Kv1 inhibitors derived from the venom of *Dendroaspis* snakes (Dolly et al., 1984; Rehm and Lazdunski, 1988; Parcej and Dolly, 1989). Currently, seven pore-forming  $\alpha$ -subunits Kv1.1–1.7 have been cloned (Gutman and Chandy, 1993) and studied in various heterologous expression systems revealing substantial differences in activation and inactivation kinetics (Baranauskas, 2007). In addition, auxiliary  $\beta$ -subunits such as Kv $\beta$ 1–3 with splice variants were discovered which may modify gating properties or serve as chaperones (Rettig et al., 1994; Scott et al., 1994; England et al., 1995; Heinemann et al., 1995; Majumder et al., 1995). The complexity of gating properties, in particular of Kv1.2, is further increased by two different activation kinetics referred to as “slow” and “fast” gating channels (Rezazadeh et al., 2007) and, finally, by glycosylation of the extracellular S1–S2 linker resulting in a

**FIGURE 5 |** Continued

Kaplan–Meier log-rank test) as well as between anti-CASPR2 and control ( $*P = 0.05$ , Kaplan–Meier log-rank test). **(E)** Onset of polyspike discharges when they were present. The difference in polyspike discharge onset was still significant between anti-Kv1.2 and control ( $+P = 0.095$ ,  $*P < 0.05$ , Mann–Whitney  $U$  test).

depolarizing shift in the half-maximal activation (Watanabe et al., 2007). Typical features of Kv1.2 are the low threshold (below action potential threshold) and the use-dependent activation (Baronas et al., 2015). Thus, Kv1.2 is activated before the action potential is elicited, and repetitive firing may increase Kv1.2 contribution to AP repolarization. It is well established that Kv1.2 is predominantly expressed at presynaptic terminals (Wang et al., 1993, 1994; Sheng et al., 1994; Monaghan et al., 2001; Gu et al., 2003; Wenzel et al., 2007; Lorincz and Nusser, 2008), but functional characterization of presynaptic ion channels is feasible only at highly specialized synapses such as the Calyx of Held (Rezazadeh et al., 2007). While it is actually impossible to predict the effects of antibodies against Kv1.2 at a certain synapse, the available data indicate that Kv1.2 powerfully counteracts depolarizing afterpotentials and thereby constrains transmitter release (Lambe and Aghajanian, 2001; Dodson et al., 2003).

What can we learn from the effects of the patient's antibody against Kv1.2? We found that Schaffer collateral-CA1, but not medial perforant path-dentate gyrus synapses showed an increased slope of the fEPSP suggesting higher synchronization of transmitter release. In the view of the role of Kv1.2 at presynaptic terminals, this implies the view that Kv1.2 antibodies may exert inhibitory effects on presynaptic Kv1.2 function which was confirmed by the significant reduction of the PPR. A similar finding was obtained from rats after intracerebroventricular injection of Kv1.4-antisense oligodeoxyribonucleotides which led to a reduced PPR and, in addition, impaired LTP in CA1 (Meiri et al., 1998). The latter, however, is difficult to explain, since reduced paired-pulse plasticity should imply an increase of transmitter release probability due to the reduction of presynaptic Kv1.4 channel function. Possibly, LTP in that study was reduced by a concomitant impairment of AMPA receptors as recently reported for anti-LGI1 (Petit-Pedrol et al., 2018). Nonetheless, increased release probability should facilitate postsynaptic depolarization and thereby LTP. In the present study, NMDAR-dependent and NMDAR-independent LTP both relying on postsynaptic depolarization were indeed enhanced in anti-Kv1.2-treated tissue in the present study. Interestingly, LTP in the dentate gyrus was preserved in both the present anti-Kv1.2 model and the Kv1.4-antisense rat (Meiri et al., 1998). Hence, anti-Kv1.2 appears to negatively interfere with presynaptic Kv1.2 function. However, the precise epitope of the antibody and consequently its molecular effects remain open, since antibody binding might affect activation, inactivation or even recovery from inactivation. The latter, for instance, is extremely slow in D-type  $K^+$  currents (Storm, 1988).

Similar to anti-Kv1.2, experiments with anti-CASPR2 showed an increased slope of the fEPSP in CA1, but not in the dentate gyrus. However, in contrast to Kv1.2, anti-CASPR2 did not

significantly reduce the PPR and, moreover, LTP values were indistinguishable from control values. These data indicate that antibodies against CASPR2 which is crucial for axonal targeting of Kv1.2 (Pinatel et al., 2017), does not seem to interfere with presynaptic Kv1.2 function. In addition, these experiments also help argue against putatively unspecific effects of the anti-Kv1.2 patient's serum, since all data on postsynaptic CA1 action potential firing properties did not differ between control and anti-CASPR2 tissues. It is, however, obvious that we cannot fully exclude that the patient's serum might contain further agents such as propofol or levetiracetam, but it is unlikely that these compounds would depress  $K^+$  channel function. A further line of evidence against unspecific effects of anti-Kv1.2 serum derives from the differential effects of this antibody on CA1 and the dentate gyrus. In fact, it was an unexpected and intriguing finding that the changes were restricted to the Schaffer collateral-CA1 synapse. This might be explained by the high diversity of Kv1.2 channel-complexes with auxiliary  $\beta$ -subunits. In this sense, it is important to note that the extracellular S1-S2 linker glycosylation is a relevant regulator of Kv1.2 activation (Watanabe et al., 2007), and N-glycosylation was required for the epitope retrieval of patient-derived antibodies in NMDAR encephalitis (Gleichman et al., 2012). Alternatively, it is also possible that the patient's antibody binds to the VGKC-complex as a whole rather than exclusively the pore-forming  $\alpha$ -subunit as previously shown for other VGKC-complex antibody species (Irani et al., 2010; Lai et al., 2010).

It has been shown that Kv1.2 is expressed on CA1 pyramidal cells, but not on dentate granule cells (Sheng et al., 1994; Guan et al., 2006). Therefore, Kv1.2 might contribute to the RMP as well as the action potential (AP) threshold and repolarization. Intracellular recordings from CA1 neurons, however, failed to detect differences in the RMP or AP characteristics such as threshold, amplitude or duration suggesting that Kv1.2 may only play a minor role under resting conditions. In addition, this may also reflect the predominantly dendritic expression of Kv1.2 (Sheng et al., 1994; Guan et al., 2006). In contrast, during prolonged depolarization CA1 neurons from anti-Kv1.2-treated rats showed a delayed onset of the first AP as well as reduced numbers of action potentials. Importantly, the latter finding refers to the original description of D-type  $K^+$  currents:  $K^+$  currents with activation thresholds below the AP threshold which therefore delayed the firing were called D-type (i.e., delay-type) (Storm, 1988). In line with this finding, the interspike interval during prolonged depolarization was significantly increased in anti-Kv1.2 tissue. It is important to note that all these findings were specific for anti-Kv1.2, since cells from anti-CASPR2-treated animals showed the same results as controls and therefore significantly differed from cells recorded in anti-Kv1.2 tissue. At first sight, the anti-Kv1.2 effects may suggest facilitated hyperpolarization rather than inhibited  $K^+$  outward currents. This is difficult to appreciate because differential effects would have to be proposed for the same antibody. However, Kv1.2 channels can be divided into slow and fast gating channels (Rezazadeh et al., 2007), and it is uncertain to what extent gating properties observed in expression systems can be transferred to presynaptic terminals. But for the dendritic Kv1.2 channels

together with the use-dependent activation of Kv1.2 (Baronas et al., 2015), it is possible that the patient's antibody shifts the slow gating channel into the fast gating one. Interestingly, both loss-of-function and gain-of-function mutations of the Kv1.2-encoding gene, KCNA2, were associated with epileptic encephalopathy (Syrbe et al., 2015). This suggests that both hyper- and hypofunction of Kv1.2 can lead to hyperexcitability.

Lastly, we also tested the tissue susceptibility to hyperexcitable states. We found that epileptic events were not significantly different between anti-Kv1.2 and both control groups. However, polyspike discharges occurred significantly earlier and with higher incidence rates in tissue from anti-Kv1.2-treated animals. Intriguingly, anti-CASPR2 tissue also showed higher rates of polyspike discharges, and, even more important, presented with seizure-like events. Together, both patient sera converted the tissue to become more vulnerable to pro-epileptic conditions. Nonetheless, the network changes in anti-Kv1.2 tissue with respect to hyperexcitability were obviously less pronounced when compared to the pre- and postsynaptic changes at Schaffer collateral-CA1 synapses as described before. This could be due to anti-Kv1.2 effects in opposite directions as observed with prolonged depolarizations in intracellular recordings, in particular with respect to hyperexcitability following both hyper- and hypofunction of KCNA2 mutations (Syrbe et al., 2015). In addition, this may also partially be attributed to the fact that Kv1.2 plays a minor role at perforant path-dentate gyrus synapses (present study) as well as at CA3 synapses (Sheng et al., 1994; Prüss et al., 2010).

What can we learn for patient care from these studies? Although it may be uncertain whether the patient's Kv1.2 antibody binds Kv1.2 directly or not, Kv1.2 appears crucial for governing excitability in the CNS. As known from knockout studies, Kv1.2 deletion is lethal within early postnatal stages, and contrasts with mild consequences of knocking out most other Kv1 channels (London et al., 1998; Smart et al., 1998; Brew et al., 2007), although Kv1.1 is much more widely expressed in the hippocampus than Kv1.2 (Wang et al., 1993, 1994; Veh et al., 1995; Grigg et al., 2000). Nonetheless, Kv1.1 and Kv1.2 are predominant target structures of autoimmune pathology in LE and Morvan syndrome (Kleopa et al., 2006). Hence, our studies can help distinguish clinically relevant autoantibodies from those representing rather as an epiphenomenon such as anti-GAD65 (Stemmler et al., 2015; Widman et al., 2015; Hackert et al., 2016). Moreover, the present study showed that anti-Kv1.2 and anti-CASPR2 differed in their cellular effects, but both led to hyperexcitability. In this sense, both patients' antibodies should be regarded as pathophysiologically relevant which is in line with previous studies on VGKC complex-antibodies (Lalic et al., 2011; Petit-Pedrol et al., 2018) and thereby give *in vitro* evidence for the clinical decision to use plasmapheresis in the present case.

## DATA AVAILABILITY STATEMENT

The datasets generated for this study are available on request to the corresponding author.

## ETHICS STATEMENT

The studies involving human participants were reviewed and approved by the Ethikkommission der Universität Rostock. The patients/participants provided their written informed consent to participate in this study. The animal study was reviewed and approved by the Landesamt für Lebensmittel, Landwirtschaft und Fischerei Mecklenburg-Vorpommern 7221.3-1.1-017/11 and 7221.3-1.1-007/16. Written informed consent was obtained from the individual(s) for the publication of any potentially identifiable images or data included in this article.

## AUTHOR CONTRIBUTIONS

HB, SK, AG, MW, SS, and AS collected the patient data. TK, ES, GH-G, JB, XG, SM, KP, and TS performed the experiments. TK, AG, MW, SS, AS, and RK contributed conception and design of the study. TK, ES, and GH-G organized the database. TK, XG,

D-CH, and KP performed the statistical analysis. TK wrote the first draft of the manuscript. AG, MW, SS, AS, and RK wrote sections of the manuscript. SM, HB, SK, and KP contributed to manuscript preparation. All authors contributed to manuscript revision, read and approved the final version of this manuscript for submission.

## FUNDING

This work was supported by a grant from the Medical Faculty of the University of Rostock to TK.

## ACKNOWLEDGMENTS

The authors wish to thank Hanka Schmidt, Simone Rackow, Andreas Prestel, and Bernd Memmner for excellent technical assistance.

## REFERENCES

- Baranauskas, G. (2007). Ionic channel function in action potential generation: current perspective. *Mol. Neurobiol.* 35, 129–150. doi: 10.1007/s12035-007-8001-0
- Baronas, V. A., McGuinness, B. R., Brigidi, G. S., Kolisko, R. N. G., Vilin, Y. Y., Kim, R. Y., et al. (2015). Use-dependent activation of neuronal Kv1.2 channel complexes. *J. Neurosci.* 35, 3515–3524. doi: 10.1523/jneurosci.4518-13.2015
- Blome, R., Bach, W., Guli, X., Porath, K., Sellmann, T., Bien, C. G., et al. (2018). Differentially altered NMDAR dependent and independent long-term potentiation in the CA3 subfield in a model of anti-NMDAR encephalitis. *Front. Synaptic Neurosci.* 31:26. doi: 10.3389/fnsyn.2018.00026
- Brew, H. M., Gittelman, J. X., Silverstein, R. S., Hanks, T. D., Demas, V. P., Robinson, L. C., et al. (2007). Seizures and reduced life span in mice lacking the potassium channel subunit Kv1.2, but hypoexcitability and enlarged Kv1 currents in auditory neurons. *J. Neurophysiol.* 98, 1501–1525. doi: 10.1152/jn.00640.2006
- Buckley, C., Oger, J., Clover, L., Tüzün, E., Carpenter, K., Jackson, M., et al. (2001). Potassium channel antibodies in two patients with reversible limbic encephalitis. *Ann. Neurol.* 50, 73–78. doi: 10.1002/ana.1097
- Cudmore, R. H., Fronzaroli-Molinieres, L., Giraud, P., and Debanne, D. (2010). Spike-time precision and network synchrony are controlled by the homeostatic regulation of the D-type potassium current. *J. Neurosci.* 30, 12885–12895. doi: 10.1523/JNEUROSCI.0740-10.2010
- Dietrich, D., Beck, H., Kral, T., Clusmann, H., Elger, C. E., and Schramm, J. (1997). Metabotropic glutamate receptors modulate synaptic transmission in the perforant path: pharmacology and localization of two distinct receptors. *Brain Res.* 767, 220–227. doi: 10.1016/s0006-8993(97)00579-9
- Dodson, P. D., Billups, B., Rusznák, Z., Szűcs, G., Barker, M. C., and Forsythe, I. D. (2003). Presynaptic rat Kv1.2 channels suppress synaptic terminal hyperexcitability following action potential invasion. *J. Physiol.* 550, 27–33. doi: 10.1113/jphysiol.2003.046250
- Dolly, J. O., Halliwell, J. V., Black, J. D., Williams, R. S., Pelchen-Matthews, A., Breeze, A. L., et al. (1984). Botulinum neurotoxin and dendrotoxin as probes for studies on transmitter release. *J. Physiol.* 79, 280–303.
- England, S. K., Uebele, V. N., Kodali, J., Bennett, P. B., and Tamkun, M. M. (1995). A novel K<sup>+</sup> channel beta-subunit (hKv beta 1.3) is produced via alternative mRNA splicings. *J. Biol. Chem.* 270, 28531–28534. doi: 10.1074/jbc.270.48.28531
- Gleichman, A. J., Spruce, L. A., Dalmau, J., Seeholzer, S. H., and Lynch, D. R. (2012). Anti-NMDA receptor encephalitis antibody binding is dependent on amino acid identity of a small region within the GluN1 amino terminal domain. *J. Neurosci.* 32, 11082–11094. doi: 10.1523/jneurosci.0064-12.2012
- Golding, N. L., Jung, H., Mickus, T., and Spruston, N. (1999). Dendritic calcium spike initiation and repolarization are controlled by distinct potassium channel subtypes in CA1 pyramidal neurons. *J. Neurosci.* 19, 8789–8798. doi: 10.1523/jneurosci.19-20-08789.1999
- Grigg, J. J., Brew, H. M., and Tempel, B. L. (2000). Differential expression of voltage-gated potassium channel genes in auditory nuclei of the mouse brainstem. *Hear. Res.* 140, 77–90. doi: 10.1016/s0378-5955(99)00187-2
- Gu, C., Jan, Y. N., and Jan, L. Y. (2003). A conserved domain in axonal targeting of Kv1 (Shaker) voltage-gated potassium channels. *Science* 301, 646–649. doi: 10.1126/science.1086998
- Guan, D., Lee, J. C. F., Tkatch, T., Surmeier, D. J., Armstrong, W. E., and Foehring, R. C. (2006). Expression and biophysical properties of Kv1 channels in supragranular neocortical pyramidal neurons. *J. Physiol.* 571, 371–389. doi: 10.1113/jphysiol.2005.097006
- Gutman, G. A., and Chandy, K. G. (1993). Nomenclature of mammalian voltage-dependent potassium channel genes. *Semin. Neurosci.* 5, 101–106. doi: 10.1016/s1044-5765(05)80004-1
- Hackert, J. K., Müller, L., Rohde, M., Bien, C. G., Köhling, R., and Kirschstein, T. (2016). Anti-GAD65 containing cerebrospinal fluid does not alter GABAergic transmission. *Front. Cell. Neurosci.* 10:130. doi: 10.3389/fncel.2016.00130
- Hart, I. K., Maddison, P., Newsom-Davis, J., Vincent, A., and Mills, K. R. (2002). Phenotypic variants of autoimmune peripheral nerve hyperexcitability. *Brain* 125(Pt. 8), 1887–1895. doi: 10.1093/brain/awf178
- Heinemann, S. H., Rettig, J., Wunder, F., and Pongs, O. (1995). Molecular and functional characterization of a rat brain Kv beta 3 potassium channel subunit. *FEBS Lett.* 377, 383–389. doi: 10.1016/0014-5793(95)01377-6
- Irani, S. R., Alexander, S., Waters, P., Kleopa, K. A., Pettingill, P., Zuliani, L., et al. (2010). Antibodies to Kv1 potassium channel-complex proteins leucine-rich, glioma inactivated 1 protein and contactin-associated protein-2 in limbic encephalitis, Morvan's syndrome and acquired neuromyotonia. *Brain* 133, 2734–2748. doi: 10.1093/brain/awq213
- Kersten, M., Rabbe, T., Blome, R., Porath, K., Sellmann, T., Bien, C. G., et al. (2019). Novel object recognition in rats with NMDAR dysfunction in CA1 after stereotactic injection of anti-NMDAR encephalitis cerebrospinal fluid. *Front. Neurol.* 10:586. doi: 10.3389/fneur.2019.00586
- Kleopa, K. A., Elman, L. B., Lang, B., Vincent, A., and Scherer, S. S. (2006). Neuromyotonia and limbic encephalitis sera target mature Shaker-type K<sup>+</sup> channels: subunit specificity correlates with clinical manifestations. *Brain* 129, 1570–1584. doi: 10.1093/brain/awl084
- Lai, M., Huijbers, M. G., Lancaster, E., Graus, F., Bataller, L., Balice-Gordon, R., et al. (2010). Investigation of LGI1 as the antigen in limbic encephalitis previously attributed to potassium channels: a case series. *Lancet Neurol.* 9, 776–785. doi: 10.1016/S1474-4422(10)70137-X

- Lalic, T., Pettingill, P., Vincent, A., and Capogna, M. (2011). Human limbic encephalitis serum enhances hippocampal mossy fiber-CA3 pyramidal cell synaptic transmission. *Epilepsia* 52, 121–131. doi: 10.1111/j.1528-1167.2010.02756.x
- Lambe, E. K., and Aghajanian, G. K. (2001). The role of Kv1.2-containing potassium channels in serotonin-induced glutamate release from thalamocortical terminals in rat frontal cortex. *J. Neurosci.* 21, 9955–9963. doi: 10.1523/jneurosci.21-24-09955.2001
- Lang, B., Makuch, M., Moloney, T., Dettmann, I., Mindorf, S., Probst, C., et al. (2017). Intracellular and non-neuronal targets of voltage-gated potassium channel complex antibodies. *J. Neurol. Neurosurg. Psychiatry* 88, 353–361. doi: 10.1136/jnnp-2016-314758
- London, B., Wang, D. W., Hill, J. A., and Bennett, P. B. (1998). The transient outward current in mice lacking the potassium channel gene Kv1.4. *J. Physiol.* 509, 171–182. doi: 10.1111/j.1469-7793.1998.171bo.x
- Lorincz, A., and Nusser, Z. (2008). Cell-type-dependent molecular composition of the axon initial segment. *J. Neurosci.* 28, 14329–14340. doi: 10.1523/JNEUROSCI.4833-08.2008
- Majumder, K., Debiasi, M., Wang, Z. G., and Wible, B. A. (1995). Molecular-cloning and functional expression of a novel potassium channel beta-subunit from human atrium. *FEBS Lett.* 361, 13–16. doi: 10.1016/0014-5793(95)00120-x
- Meiri, N., Sun, M.-K., Segal, Z., and Alkon, D. L. (1998). Memory and long-term potentiation (LTP) dissociated: normal spatial memory despite CA1 LTP elimination with Kv1.4 antisense. *Proc. Natl. Acad. Sci. U.S.A.* 95, 15037–15042. doi: 10.1073/pnas.95.25.15037
- Mitterdorfer, J., and Bean, B. P. (2002). Potassium currents during the action potential of hippocampal CA3 neurons. *J. Neurosci.* 22, 10106–10115. doi: 10.1523/jneurosci.22-23-10106.2002
- Monaghan, M. M., Trimmer, J. S., and Rhodes, K. J. (2001). Experimental Localization of Kv1 Family Voltage-Gated K<sup>+</sup> Channel  $\alpha$  and  $\beta$  Subunits in Rat Hippocampal Formation. *J. Neurosci.* 21, 5973–5983. doi: 10.1523/jneurosci.21-16-05973.2001
- Parcej, D. N., and Dolly, J. O. (1989). Dendrotoxin acceptor from bovine synaptic plasma membranes: binding properties, purification and subunit composition of a putative constituent of certain voltage-activated K<sup>+</sup> channels. *Biochem. J.* 257, 899–903. doi: 10.1042/bj2570899
- Petit-Pedrol, M., Sell, J., Planagumà, J., Mannara, F., Radosevic, M., Haselmann, H., et al. (2018). LGI1 antibodies alter Kv1.1 and AMPA receptors changing synaptic excitability, plasticity and memory. *Brain* 141, 3144–3159. doi: 10.1093/brain/awy253
- Pinatel, D., Hivert, B., Saint-Martin, M., Noraz, N., Savvaki, M., Karageorgos, D., et al. (2017). The Kv1-associated molecules TAG-1 and Caspr2 are selectively targeted to the axon initial segment in hippocampal neurons. *J. Cell Sci.* 130, 2209–2220. doi: 10.1242/jcs.202267
- Prüss, H., Grosse, G., Brunk, I., Veh, R. W., and Ahnert-Hilger, G. (2010). Age-dependent axonal expression of potassium channel proteins during development in mouse hippocampus. *Histochem. Cell. Biol.* 33, 301–312. doi: 10.1007/s00418-009-0668-z
- Rehm, H., and Lazdunski, M. (1988). Purification and subunit structure of a putative K<sup>+</sup>-channel protein identified by its binding properties for dendrotoxin I. *Proc. Natl. Acad. Sci. U.S.A.* 85, 4919–4923. doi: 10.1073/pnas.85.13.4919
- Rettig, J., Heinemann, S. H., Wunder, F., Lorra, C., Parcej, D. N., Dolly, J. O., et al. (1994). Inactivation properties of voltage-gated K<sup>+</sup> channels altered by presence of beta-subunit. *Nature* 369, 289–294. doi: 10.1038/369289a0
- Rezazadeh, S., Kurata, H. T., Claydon, T. W., Kehl, S. J., and Fedida, D. (2007). An activation gating switch in Kv1.2 is localized to a threonine residue in the S2-S3 LINKER. *Biophys. J.* 93, 4173–4186. doi: 10.1529/biophysj.107.116160
- Scott, V. E. S., Rettig, J., Parcej, D. N., Keen, J. N., Findlay, J. B. C., Pongs, O., et al. (1994). Primary structure of a beta subunit of alpha-dendrotoxin-sensitive K<sup>+</sup> channels from bovine brain. *Proc. Natl. Acad. Sci. U.S.A.* 91, 1637–1641. doi: 10.1073/pnas.91.5.1637
- Sheng, M., Tsaur, M. L., Jan, Y. N., and Jan, L. Y. (1994). Contrasting subcellular localization of the Kv1.2 K<sup>+</sup> channel subunit in different neurons of rat brain. *J. Neurosci.* 14, 2408–2417. doi: 10.1523/jneurosci.14-04-02408.1994
- Smart, S. L., Lopantsev, V., Zhang, C. L., Robbins, C. A., Wang, H., Chiu, S. Y., et al. (1998). Deletion of the K(v)1.1 potassium channel causes epilepsy in mice. *Neuron* 20, 809–819. doi: 10.1016/s0896-6273(00)81018-1
- Stemmler, N., Rohleder, K., Malter, M. P., Widman, G., Elger, C. E., Beck, H., et al. (2015). Serum from a patient with GAD65 antibody-associated limbic encephalitis did not alter GABAergic neurotransmission in cultured hippocampal networks. *Front. Neurol.* 6:189. doi: 10.3389/fneur.2015.00189
- Storm, J. F. (1988). Temporal integration by a slowly inactivating K<sup>+</sup> current in hippocampal neurons. *Nature* 336, 379–381. doi: 10.1038/336379a0
- Stühmer, W., Ruppersberg, J. P., Schröter, K. H., Sakmann, B., Stocker, M., Giese, K. P., et al. (1989). Molecular basis of functional diversity of voltage gated potassium channels in mammalian brain. *EMBO J.* 8, 3235–3244. doi: 10.1002/j.1460-2075.1989.tb08483.x
- Syrbe, S., Hedrich, U. B. S., Riesch, E., Djémié, T., Müller, S., Möller, R. S., et al. (2015). De novo loss- or gain-of-function mutations in KCNA2 cause epileptic encephalopathy. *Nat. Genet.* 47, 393–399. doi: 10.1038/ng.3239
- Syrbe, S., Stettner, G. M., Bally, J., Borggraeve, I., Bien, C. I., Ferfaglia, R. I., et al. (2020). CASPR2-autoimmunity in children, expanding to mild encephalopathy with hypertension. *Neurology*. [in press].
- Veh, R. W., Lichtinghagen, R., Sewing, S., Wunder, F., Grumbach, I. M., and Pongs, O. (1995). Immunohistochemical localization of five members of the Kv1 channel subunits: contrasting subcellular locations and neuron-specific colocalizations in rat brain. *Eur. J. Neurosci.* 7, 2189–2205. doi: 10.1111/j.1460-9568.1995.tb00641.x
- Wang, H., Kunkel, D. D., Martin, T. M., Schwartzkroin, P. A., and Tempel, B. L. (1993). Heteromultimeric K<sup>+</sup> channels in terminal and juxtaparanodal regions of neurons. *Nature* 365, 75–79. doi: 10.1038/365075a0
- Wang, H., Kunkel, D. D., Schwartzkroin, P. A., and Tempel, B. L. (1994). Localization of Kv1.1 and Kv1.2, two K channel proteins, to synaptic terminals, somata and dendrites in the mouse brain. *J. Neurosci.* 14, 4588–4599. doi: 10.1523/jneurosci.14-08-04588.1994
- Watanabe, I., Zhu, J., Sutachan, J. J., Gottschalk, A., Recio-Pinto, E., and Thornhill, W. B. (2007). The glycosylation state of Kv1.2 potassium channels affects trafficking, gating, and simulated action potentials. *Brain Res.* 1144, 1–18. doi: 10.1016/j.brainres.2007.01.092
- Wenzel, H. J., Vacher, H., Clark, E., Trimmer, J. S., Lee, A. L., Sapolsky, R. M., et al. (2007). Structural consequences of Kcna1 gene deletion and transfer in the mouse hippocampus. *Epilepsia* 48, 2023–2046. doi: 10.1111/j.1528-1167.2007.01189.x
- Widman, G., Golombeck, K., Hautzel, H., Gross, C. C., Quesada, C. M., Witt, J. A., et al. (2015). Treating a GAD65 antibody-associated limbic encephalitis with Basiliximab: a case study. *Front. Neurol.* 6:167. doi: 10.3389/fneur.2015.00167
- Würdemann, T., Kersten, M., Tokay, T., Guli, X., Kober, M., Rohde, M., et al. (2016). Stereotactic injection of cerebrospinal fluid from anti-NMDA receptor encephalitis into rat dentate gyrus impairs NMDA receptor function. *Brain Res.* 1633, 10–18. doi: 10.1016/j.brainres.2015.12.027
- Zucker, R. S. (2002). Short-term plasticity. *Annu. Rev. Physiol.* 64, 355–405. doi: 10.1146/annurev.physiol.64.092501.114547

**Conflict of Interest:** The authors declare that the research was conducted in the absence of any commercial or financial relationships that could be construed as a potential conflict of interest.

Copyright © 2020 Kirschstein, Sadkiewicz, Hund-Göschel, Becker, Guli, Müller, Rohde, Hübner, Brehme, Kolbaske, Porath, Sellmann, Großmann, Wittstock, Syrbe, Storch and Köhling. This is an open-access article distributed under the terms of the Creative Commons Attribution License (CC BY). The use, distribution or reproduction in other forums is permitted, provided the original author(s) and the copyright owner(s) are credited and that the original publication in this journal is cited, in accordance with accepted academic practice. No use, distribution or reproduction is permitted which does not comply with these terms.